for gastrointestinal cancer in the clinical setting. The successful elimination of sentinel lymph node metastasis indicates that concurrent submucosal injection of OBP-301 and endoscopic tumor removal might be a paradigm-changing therapeutic alternative to prophylactic surgery for patients with submucosally invaded gastrointestinal cancer.

RESULTS

In vitro cytopathic effect of the virus on human colorectal cancer cells

OBP-301 (Telomelysin) is an attenuated adenovirus that drives the *E1A* and *E1B* genes under the human telomerase reverse transcriptase (hTERT) promoter and is capable of killing human epithelial as well as mesenchymal malignant cells in a telomerase-dependent manner (**Supplementary Figure S1a**).[19–21] To assess the cytopathic effect (CPE) of OBP-301 on human colorectal cancer cells, green fluorescent protein (GFP)-labeled HCT-116 or Colo 205 cells were infected either with OBP-301 or with a replication-deficient, E1-deleted adenovirus, dl312 and were photographed using a fluorescent microscope after viral infection. Both HCT-116-GFP and Colo 205-GFP cells infected with OBP-301 at an MOI of 10 exhibited rapid cell death by 72 hours after virus infection, whereas cells treated with the same MOI of dl312 or with PBS showed no morphological change (**Figure 1a** and **Supplementary Figure S2**). The XTT cell-viability assay also demonstrated that OBP-301 infection induced cell death in a dose-dependent fashion both in HCT-116-GFP and Colo 205-GFP cells, whereas infection with dl312 did not show significant CPE at multiplicity of infections (MOIs) of up to 100 (**Figure 1b**). We previously reported that no apparent CPE was observed in normal human cell lines after OBP-301 infection.[19]

Sentinel lymph node metastasis in an orthotopic rectal cancer xenograft model

A submucosally invaded early rectal tumor model was established by inoculating HCT-116-GFP or Colo205-GFP human colorectal cancer cells orthotopically into athymic *nu/nu* mice. Seven days after implantation of GFP-labeled cancer cells into the submucosal layer of the rectum, the mice developed minute rectal tumors that were clearly visible by fluorescence imaging of GFP signals (**Figure 2a**, **Supplementary Figures S3 and S5a**). Histopathological examination of the excised primary rectal tumors showed submucosal tumor formation composed of implanted cancer cells with no muscularis propria invasion. Examination under high magnification showed cancer cell-filled lymphatic vessels in the submucosal layer (**Figure 2b**). The metastatic status of regional lymph nodes was easily assessed at laparotomy, by detection of cancer cell-derived GFP signals in the lymph node (**Figure 2c,d**). A series of experiments confirmed that the percent metastasis to the sentinel lymph node on day 7 after tumor cell inoculation in mice implanted with HCT-116-GFP or Colo 205-GFP was 78.5% (33/42) and 62.5% (25/40), respectively.

Viral trafficking to lymph nodes and selective replication in metastatic foci

The lymphatic system is a major pathway for the metastatic spread of cancers as well as for the regional distribution of

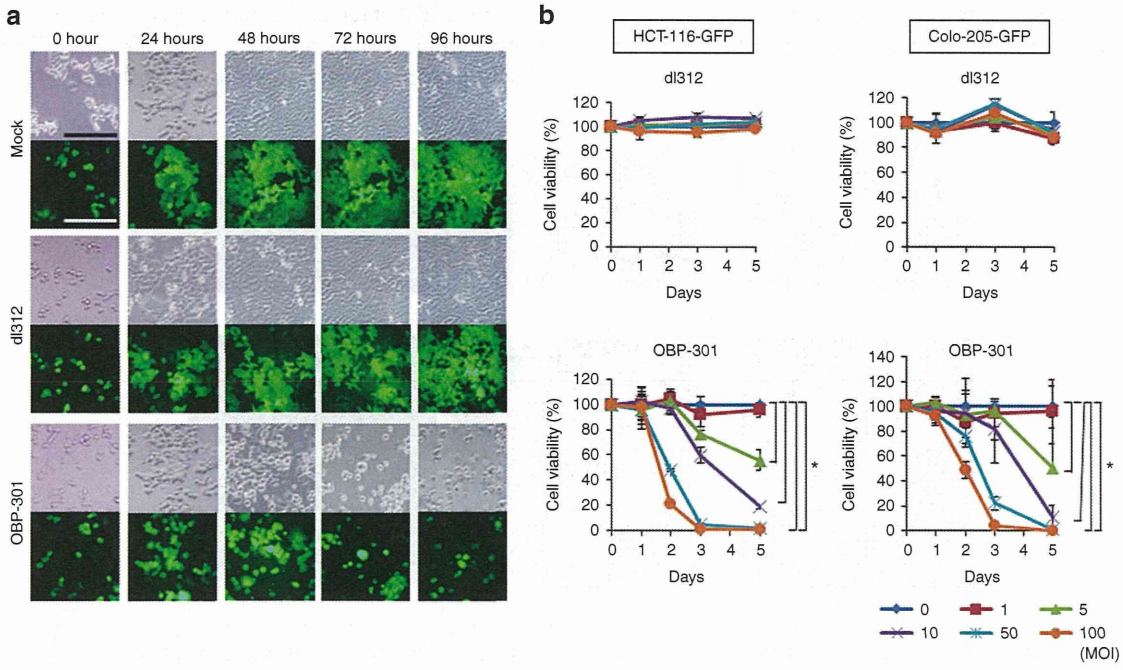

Figure 1 Cytopathic effect of OBP-301 on human colorectal cancer cell lines. (**a**) HCT-116-GFP cells were infected with replication-deficient adenovirus dl312 or OBP-301 at a multiplicity of injection (MOI) of 10. Cell morphology and GFP expression were evaluated at the indicated time points by phase-contrast (top panels) and fluorescence (bottom panels) microscopy, respectively. Magnification: ×200. Scale bar, 200 μm. (**b**) HCT-116-GFP and Colo 205-GFP cells were infected with OBP-301 or dl312 at the indicated MOIs and cell survival was quantified over 5 days using the XTT assay. The cell viability of a mock-treated group on each day was considered 100% and the percent cell viability was calculated. Data are means ± SD. Statistical significance was defined as $^*P < 0.05$.

biological mediators including fluids, proteins, chemicals, cells and drugs. Prior to injection of virus, we first assayed the ability of an injected solution to reach the draining lymph nodes. For this purpose, we investigated the diffusion pattern of a 1% indigo-carmine-blue dye solution that was peritumorally injected into the submucosal space of the rectum in the orthotopic rectal cancer mouse models. Intense blue staining was detected in regional lymph nodes as early as 1 minute after injection of the dye, indicating that an injected solution could rapidly enter the lymphatics and spread to the draining lymph nodes (**Supplementary Figure S4**).

To verify that virus could move to regional lymph nodes and further infect tumor cells in these nodes after peritumoral injection into the submucosal space of the mouse rectum, we used RFP-labeled HCT-116 cells and GFP-expressing OBP-401 (TelomeScan). OBP-401 was constructed by inserting the *GFP* gene under the control of the cytomegalovirus promoter at the deleted E3 region of OBP-301 (ref. [13,22]) (**Supplementary Figure S1**). When RFP-expressing sentinel lymph node metastases were established, mice were peritumorally injected with OBP-401 into the rectal submucosal space. Six days after OBP-401 injection, virus-induced GFP expression was detected in the sentinel lymph nodes by fluorescence imaging. The merged images showed that the viral GFP signals were coincident with RFP fluorescence of metastatic foci in sentinel lymph nodes (**Figure 3a,b**). Moreover, immunohistochemical staining for adenoviral E1A protein demonstrated that the E1A protein was selectively expressed in the metastatic area in lymph nodes, confirming the presence of replicating OBP-301 in metastatic tumor cells (**Figure 3c**). These results indicate that, after injection into the submucosal space, OBP-301 can traffic through the lymphatics to the regional lymph nodes and selectively replicate in cancer cells in metastatic lymph nodes.

Virus-mediated biological ablation of metastatic foci in regional lymph nodes

We next examined whether peritumoral submucosal injection of OBP-301 followed by primary tumor resection could ablate lymph node metastasis in the orthotopic submucosally invaded rectal cancer mouse models. Seven days after inoculation with HCT-116-GFP human colorectal cancer cells, mice that had successfully established GFP-expressing lymph node metastasis were selected by fluorescence imaging at laparotomy, and were further studied (**Figure 4a**). When primary rectal tumors were surgically removed, a solution containing OBP-301 (1×10^9 plaque forming units (PFU)/30 µl PBS) was peritumorally injected into the submucosal space as a fluid cushion. This fluid cushion was used to lift up the tumors in order to precisely preserve the rectal muscular layer (**Supplementary Figure S5**). These procedures mimicked the standard ESD technique in humans. Seven days after tumor resection, a second-look laparotomy was performed to assess tumor progression in the lymph nodes. Mice treated with PBS (30 µl), cisplatin (30 µl of concentrated original solution; 30 µg), or dl312 (1×10^9 PFU/30 µl PBS) showed more intense GFP expression, and GFP expression over a wider area in metastatic lymph nodes, whereas GFP signals were undetectable in mice that had received OBP-301, indicating the complete eradication of metastatic tumor cells in these mice (**Figure 4b**).

To more precisely quantify virus-mediated effects on lymph node metastasis, fluorescence intensities were measured using image analysis software. Preinjection of OBP-301 prior to primary tumor resection significantly reduced GFP signals compared to the other groups in both the HCT-116 and Colo 205 mouse models (**Figure 5a**). Quantification of the amounts of human cancer cells in mouse lymph nodes by using a highly sensitive real-time PCR method that targets human *Alu* sequences also demonstrated that OBP-301 completely eradicated metastatic human cancer cells (**Figure 5b**). Furthermore, lower viral doses (1×10^7 or 1×10^6

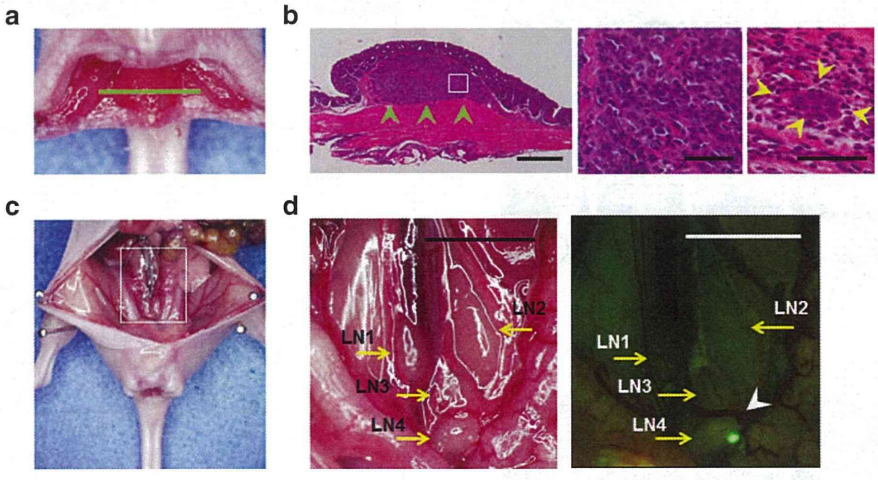

Figure 2 Submucosally invaded orthotopic xenografts of human colorectal cancer cells and subsequent development of sentinel lymph node metastasis. HCT-116-GFP human colorectal cancer cells (1.5×10^6 cells/mouse) were submucosally inoculated into the rectum of nude mice. (**a**) Macroscopic appearance of an HCT-116-GFP rectal tumor at 7 days after tumor inoculation. Green line, direction of tumor cross-sections. (**b**) Histological sections stained with hematoxylin and eosin showing local growth of the HCT-116-GFP tumor in the submucosal layer of the rectum (green arrowheads). Scale bar, 500 µm. Left, ×40 magnification; middle, detail of the boxed region of the left panel, ×400; right, lymphatic vessel invasion of HCT-116-GFP cancer cells (yellow arrowheads), ×400 magnification. (**c**) Gross appearance of the abdominal cavity in a representative mouse. Seven days after inoculation of HCT-116-GFP cancer cells, mice were assessed for lymph node metastasis at laparotomy. The white box outlines the region shown in **d**. (**d**) Left, four para-aortic lymph nodes (LN) were identified (yellow arrows). Right, a sentinel node was positive for a light-emitting spot with GFP fluorescence expressed by HCT-116-GFP cells observed by fluorescence imaging (white arrowhead). Scale bar, 5 mm.

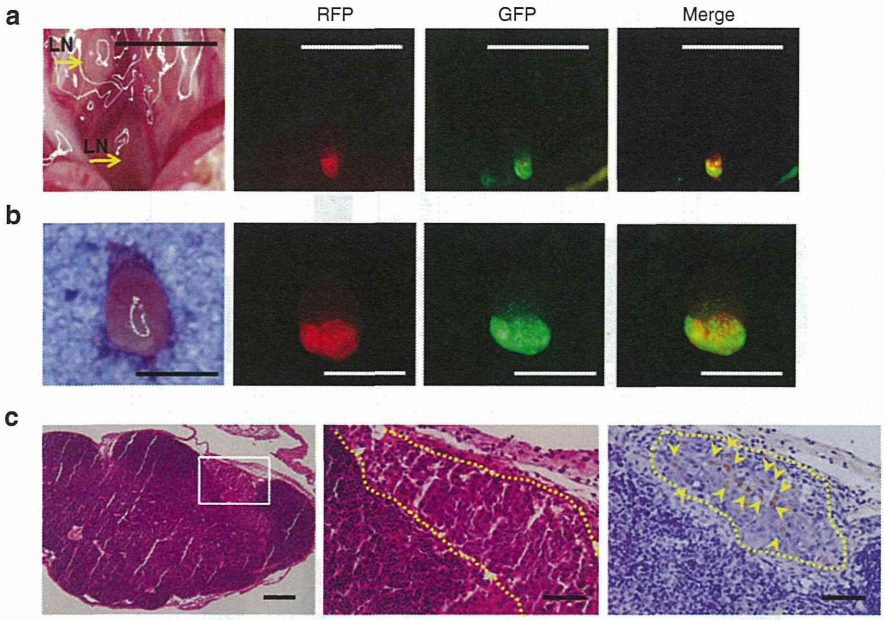

Figure 3 Lymphatic spread of the virus and selective replication in metastatic foci in regional lymph nodes. Mice bearing HCT-116-RFP primary rectal tumors that developed lymph node metastasis were peritumorally injected with 1×10^8 PFU of GFP-expressing OBP-401 into the submucosal space of the rectum. Virus spread and replication were assessed at laparotomy 6 days after virus administration. Three mice used for this study and analyses of a representative mouse are shown. (**a**) Gross localization of tumor-derived RFP and virus-induced GFP expression in the abdominal cavity of a representative mouse. The merged image shows that RFP-expressing metastatic foci in the sentinel lymph node were labeled with GFP fluorescence by OBP-401, indicating the successful delivery and replication of the virus in metastatic lymph nodes. Scale bars: 5 mm. (**b**) Excised metastatic lymph node of **a**. Scale bar: 2 mm. (**c**) Histopathological examination of excised metastatic lymph nodes. Left, hematoxylin and eosin staining showing metastatic foci. Scale bar, 200 μm; middle, detail of the boxed region of the left panel. Scale bar, 50 μm; right, immunohistochemical staining for adenoviral E1A protein in a serial section showing selective viral replication within tumor cells. The nuclei were counterstained with hematoxylin. Positive staining is reddish brown (yellow arrowheads). Scale bar, 50 μm.

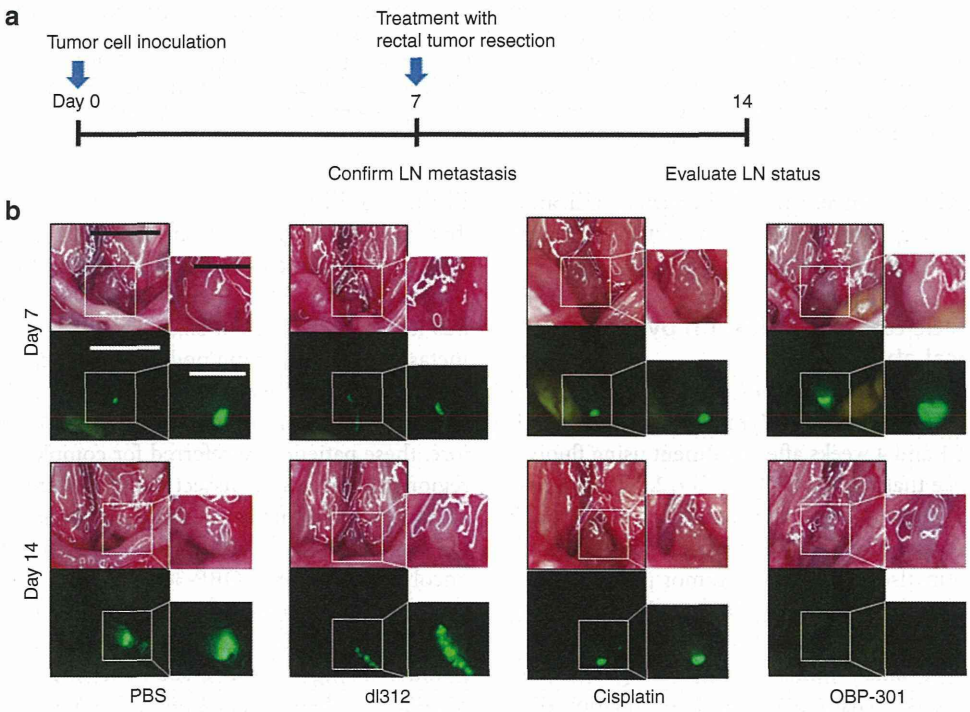

Figure 4 Biologically targeted ablation using OBP-301 eliminates metastatic foci on sentinel lymph nodes in an orthotopic colorectal cancer mouse model. (**a**) Treatment and evaluation schedule of animal experiments. (**b**) Macroscopic and fluorescence images of the abdominal cavity at laparotomy. Representative images among seven or eight mice with GFP-expressing metastatic foci in regional lymph nodes on day 7 of tumor inoculation are shown (top panels). Following treatment with mock (PBS), dl312, cisplatin, or OBP-301, the same mice were re-evaluated at laparotomy for the size and intensity of GFP signals on metastatic lymph nodes on day 14 (bottom panel). Scale bar, 5 mm (low magnification); 2 mm (high magnification).

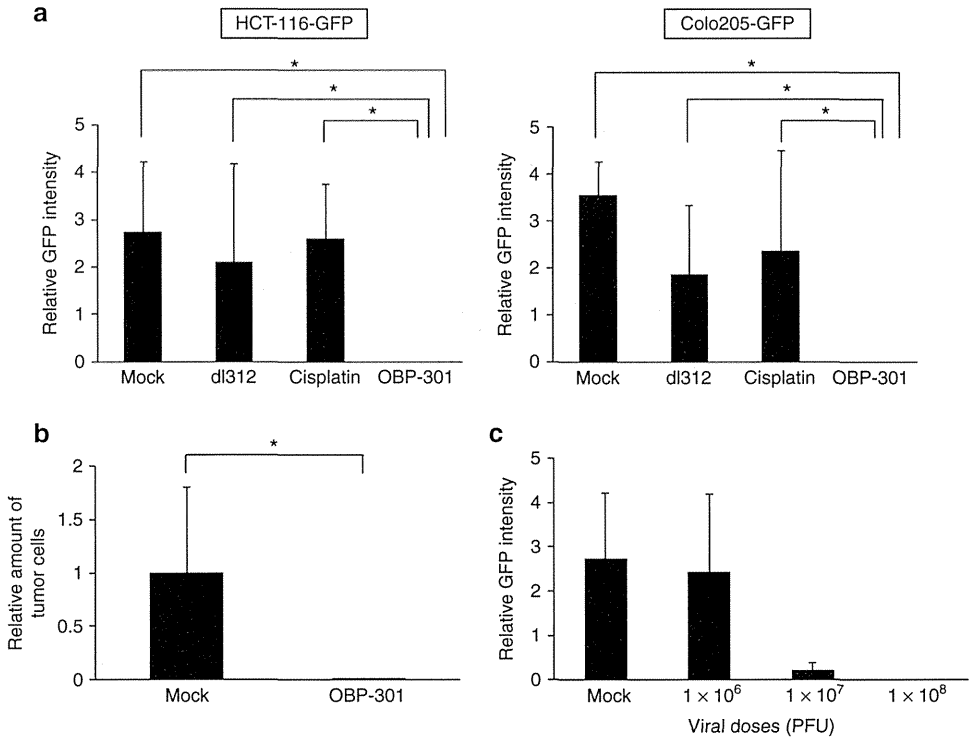

Figure 5 Quantitative analysis of the antitumor effect of OBP-301 on lymph node metastasis in an orthotopic colorectal cancer xenograft model. (**a**) The ratio of tumor cell-derived GFP intensity on metastatic lymph nodes of HCT-116-GFP (left panel) or Colo205-GFP (right panel) inoculated mice before and after the indicated treatments was calculated based on measurements of fluorescence images by using Image J software. We used seven or eight mice with Colo205-GFP cells and six mice with HCT116-GFP cells for each treatment group. Data are means ± SD. Statistical significance was defined as $P < 0.05$ (single asterisk). (**b**) Mice with established orthotopic early HCT-116-GFP tumors were treated with submucosal injection of 1×10^9 PFU of OBP-301 or dl312 followed by primary rectal tumor dissection on day 7 after tumor inoculation. Three mice were used for each group. Lymph nodes were harvested on day 14, and DNA was then extracted and subjected to quantitative *Alu* PCR analysis. The number of metastatic tumor cells is defined as the *Alu*/*GAPDH* ratio relative to that of the mock (PBS)-treated sample (mock = 1). Data are shown as means ± SD. Statistical significance was defined as $P < 0.05$ (single asterisk). (**c**) A dose-dependent purging effect of OBP-301 on metastatic lymph nodes. Mice with orthotopic early HCT-116-GFP tumors received a submucosal injection of OBP-301 at the indicated MOIs on day 7 and were subsequently subjected to GFP image-based quantification of lymph node metastasis on day 14. The numbers of mice used in this experiment are eight (mock) and four each (viral treatments). Data are shown as means ± SD.

PFU/30 μl PBS) failed to eliminate GFP fluorescence, indicating that these virus-mediated purging effects on metastatic lymph nodes were dose-dependent (**Figure 5c**).

Sustained metastatic tumor eradication by virus-mediated biological ablation

Finally, to assess if OBP-301-mediated biological ablation exerted prolonged antitumor effects, metastatic lymph nodes were visualized at laparotomy at 1 and 4 weeks after treatment using fluorescence imaging. In mice that received PBS or dl312, all metastatic lymph nodes grew larger in a time-dependent manner, although the magnitude of the enlargement varied between individual mice. Preinjection of cisplatin also did not affect tumor progression in the lymph nodes (**Supplementary Figure S6**). On the other hand, mice pretreated with OBP-301 showed no GFP fluorescence for at least 4 weeks after primary tumor resection (**Figure 6** and **Supplementary Figure S6**). Histopathological examination confirmed that virally purged lymph nodes were relapse-free (data not shown). These results suggest that submucosal preinjection of OBP-301 followed by primary tumor resection sustainably prevented metastatic tumor relapse over a long period.

DISCUSSION

The standard of care for treatment of intramucosal neoplastic lesions of the esophagus, stomach and colorectum is now a patient-friendly ESD that enables en-block resection of cancerous lesions regardless of size, since intramucosal tumors rarely metastasize to the lymph node.[2,23–25] However, when tumors penetrate slightly deeper into the submucosal layer, the incidence of nodal metastasis appears to increase significantly and, therefore, these patients are referred for complementary surgery with regional lymph node dissection.[10,11,26] Here, we describe a more effective and less invasive biological management for lymphatic metastasis that uses the telomerase-specific, replication-selective, oncolytic adenovirus OBP-301 and that employs submucosally invaded early rectal cancer orthotopic mouse models. In place of surgical lymphadenectomy we used a solution containing a tumor-killing virus as a submucosal cushioning agent before resection of the primary tumor. From a clinical viewpoint, this new, simple, and robust strategy is a more realistic and promising bench-to-bedside translation than prophylactic surgery for ablation of potential lymph node metastases in early gastrointestinal cancer patients.

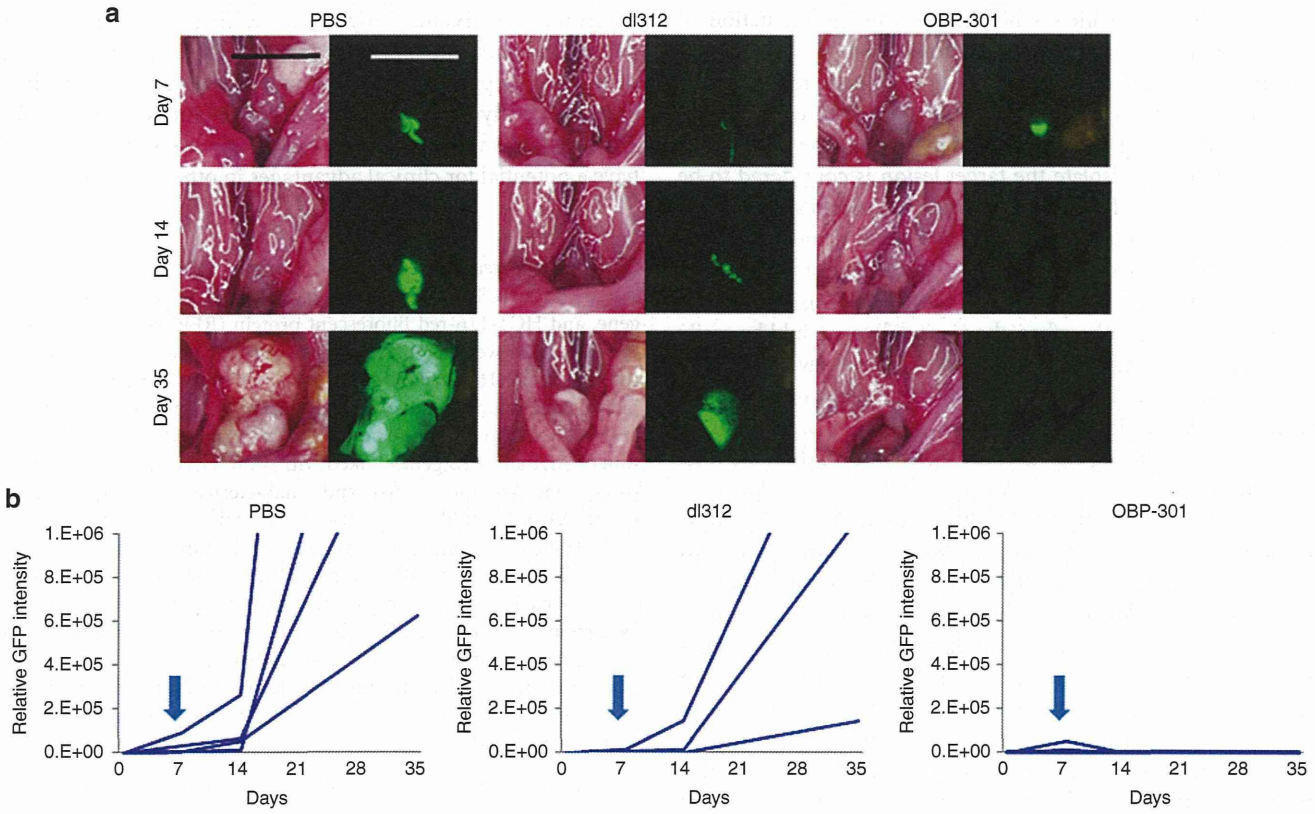

Figure 6 Virus-mediated biological elimination of established lymph node metastasis prevented relapse. (**a**) Gross and fluorescence images of the abdominal cavity were serially obtained at laparotomy on days 7, 14, and 35 after tumor inoculation in orthotopic HCT-116-GFP tumor xenografts treated with PBS, dl312, or OBP-301. Representative images of each group are shown. Scale bar, 5 mm. (**b**) The GFP intensity of metastatic lymph nodes in each mouse was serially measured on days 7, 14, and 35. Data from each mouse are plotted individually. Arrows indicate the time of virus injection and primary tumor removal.

Overexpression of telomerase, which is a ribonucleoprotein enzyme complex that is responsible for the complete replication of chromosomal ends, is thought to play a key role in the infinite reproduction of cancer cells.[27,28] We constructed a telomerase-specific replicating adenovirus, OBP-301, in which the hTERT promoter element drives expression of the *E1* genes that are essential for adenoviral replication.[19] As hTERT is the catalytic subunit of telomerase, OBP-301 shows tumor-specific intracellular viral replication that is regulated by hTERT transcriptional activity in human tumors.[19–21] Viral yields correlated well with *hTERT* mRNA expression in human cancer cell lines,[13,22] although there was no significant correlation between *hTERT* mRNA expression and the cytopathic activity of OBP-301.[21] It has been reported that the hTERT promoter could be applied to induction of transgene expression in syngeneic tumors in mice.[29] We also previously confirmed that a hTERT promoter-driven tumor-killing adenovirus could replicate in murine colorectal cancer cells such as Colon-26 *in vitro* and *in vivo*.[13] These findings suggest that OBP-301 can replicate in murine as well as in human tissues, when telomerase is activated. Thus, the submucosally invaded orthotopic early rectal cancer mouse model, which develops spontaneous lymph node metastasis, is a suitable translational animal model for simulation of the *in vivo* behavior patterns of this virus.

The lymphatic system plays a crucial role in initial lymphatic dissemination of human cancer cells and subsequent development of lymph node metastases. In addition to the pre-existing lymphatic network, it is well known that new lymphatic vessels can be generated from pre-existing ones by tumor-secreting mediators such as vascular endothelial growth factors (VEGF) and angiopoietins.[30] This tumor-induced lymphangiogenesis is often associated with structural and functional abnormalities of the lymphatic vasculature, which are analogous to the aberrations of tumor blood vessels.[31] Although lymphatic vessels began to show abnormalities even in the early stages of carcinogenesis, advanced tumors have more compressed and nonfunctional lymphatics presumably due to tumor infiltration.[32] The lymphatic system also provides a route for the delivery of therapeutic molecules including biological agents. We have shown that OBP-301 virus injected into the space under the orthotopically implanted early rectal cancer could easily reach regional lymph nodes with normal lymphatic flow. However, a complex and impaired lymphatic network in more advanced tumors might disturb an optimal distribution of therapeutics into the regional lymphatic area. Therefore, early-stage cancer patients who potentially have microlymph node metastasis might be an appropriate target for locoregional therapy through the lymphatic system.

The standard procedures for ESD, which include marking outside the lesion, injection of various submucosal solutions, circumferential incision into the mucosa and direct dissection of the submucosal layer, have been established.[33] As submucosal

dissection with simultaneous hemostasis causes destruction of the normal lymphatic network, administration of therapeutic molecules prior to complete removal of neoplastic lesions is the ideal time to deliver these molecules over the locoregional lymphatic area including the sentinel lymph nodes. The use of submucosal injection to isolate the target lesion is considered to be essential for a successful ESD. In addition to normal saline, many types of solutions such as glycerol, dextrose water, and hyaluronic acid have been applied clinically.[34] The key aspect of our study is that a solution containing tumor-killing virus was used as a submucosal cushion and, therefore, the virus delivery could be easily adapted to the standard ESD procedures. Moreover, we found that submucosally injected dye could rapidly enter the lymphatic flow and spread to the draining lymph nodes, indicating a potential for extension of the purging effects of the viruses beyond the sentinel lymph nodes.

Submucosal injection of OBP-301 prior to ESD-mimicking resection of submucosally invaded primary tumors resulted in complete inhibition of metastatic outgrowth on the draining lymph nodes in a dose-dependent manner. Replicating viruses in metastatic foci of the sentinel lymph nodes could be visualized using dual-color *in vivo* imaging. Preclinical studies have demonstrated that the antitumor efficiency of OBP-301 strongly depends on its infectivity towards tumor cells, which varies among tumor types.[21,35] However, a dose-titration study indicated that OBP-301 at 10^7 PFU, which is 2 logs lower than the optimal concentration for mice (1×10^9 PFU/mouse), could still effectively suppress lymph node metastasis, suggesting that the use of higher doses of OBP-301 could potentially overcome the varied sensitivity of tumor cells to OBP-301. The safety profile of OBP-301 itself after intratumoral delivery has already been confirmed up to 1×10^{12} virus particles (vp) (1×10^{11} PFU) in a phase 1 clinical trial for various types of solid tumors.[36] Furthermore, an investigator-driven clinical study of OBP-301 in combination with radiotherapy for esophageal cancer is currently ongoing in our hospital without any severe dose-limiting toxicity. Therefore, a 2-log-higher dose of OBP-301 could be available in humans for monotherapy as well as for combination therapy. In addition, analysis of autopsied patients in our previous trial showed that a replication-defective adenoviral vector can persist in proximal lymph nodes for ~5 months after intratumoral injection.[37] Indeed, although metastatic lymph nodes grew in mice that received cisplatin, which is a broadly used anticancer drug, no recurrence was observed in OBP-301–treated mice in which lymph node metastasis had been eradicated, suggesting a long-term surveillance activity of OBP-301.

In conclusion, we have demonstrated that the telomerase-specific replication-selective adenovirus OBP-301 can be delivered into neoplastic foci in regional lymph nodes after submucosal injection at the time of primary tumor dissection and effectively ablate lymph node metastasis in an early gastrointestinal cancer model. We previously reported that metastatic tumor cells in the lymph nodes unexpectedly increased after surgical removal of invasive rectal tumors, presumably due to excessive damage to the host[38]; however, less-invasive submucosal dissection of tumors did not affect the incidence of lymph node metastasis. The administration of OBP-301 by inclusion in the standard ESD procedures is a revolutionary treatment option for early gastrointestinal cancer patients, which avoids impairing the quality of life that occurs due to surgery for prophylactic lymphadenectomy. Moreover, clinical morbidity of lymphedema particularly in breast cancer axillary node dissection is of significant consequence. Our strategy may have a potential for clinical advantages in other oncologic fields.

MATERIALS AND METHODS

Cell lines and recombinant adenoviruses. The human colorectal cancer cell lines HCT-116-GFP and Colo 205-GFP, which express the *GFP* gene, and HCT-116-red fluorescent protein (RFP) cells, which express the *RFP* gene, were established previously,[39–42] and were routinely cultured in RPMI 1640 medium supplemented with 10% FBS. The recombinant replication-selective, tumor-specific adenovirus vector OBP-301 (Telomelysin), in which the hTERT promoter element drives the expression of *E1A* and *E1B* genes linked with an internal ribosome entry site, was previously constructed and characterized[19–21] (**Supplementary Figure S1a**). OBP-401 (TelomeScan) is a telomerase-specific, replication-competent adenovirus variant in which the replication cassette and *GFP* gene under the control of the cytomegalovirus promoter were inserted into the E3 region for monitoring of viral replication[13,22] (**Supplementary Figure S1b**). The E1A-deleted adenovirus vector lacking a cDNA insert (dl312) was also used as a control vector. Viruses were purified by ultracentrifugation using CsCl step gradients. Viral titers were determined by a plaque-forming assay using 293 cells. The virus was stored at −80 °C.

Cell viability assay. HCT-116-GFP and Colo 205-GFP cells were seeded on 96-well plates at a density of 1×10^3 cells/well 18–20 hours before viral infection. The cells were then infected with OBP-301 or control dl312 at an MOI of 0, 1, 5, 10, 50, or 100 PFU/cell. Cell viability was determined on days 1, 2, 3, and 5 after virus infection using the Cell Proliferation Kit II (Roche Molecular Biochemicals, Indianapolis, IN), which is based on a sodium 3′-[1-(phenylaminocarbonyl)-3,4-tetrazolium]-bis(4-methoxy-6-nitro)benzene sulfonic acid hydrate (XTT) assay, according to the manufacturer's protocol.

Animal experiments. The experimental protocol was approved by the Ethics Review Committee for Animal Experimentation of our institution. Six- to 8-week-old, female BALB/c nude mice (Clea Japan, Tokyo, Japan) were used in this study. All animal procedures were performed under anesthesia using s.c. administration of a ketamine mixture (100 mg/kg ketamine HCL, 7 mg/kg xylazine HCL).

Mice were anesthetized and placed in a supine position. Both the dorsal vaginal wall and the ventral ano-rectal wall were cut at a length of 7 mm to expose the rectal mucosa for an easy operation. To develop a submucosally invaded orthotopic rectal cancer model, HCT-116-GFP, Colo205-GFP, or HCT-116-RFP human colon cancer cells (1.5×10^6 cells/mouse), suspended in a mixture of 15 µl of PBS and 15 µl of Matrigel (BD Biosciences, San Jose, CA), were slowly injected into the submucosal layer of the rectum using a 30-gauge needle (**Supplementary Figure S3**). Seven days later, after fluorescent signals were confirmed in the sentinel lymph nodes at laparotomy, a 30 µl-solution containing OBP-301, OBP-401, or dl312 at the indicated doses was peritumorally injected into the submucosal space as a fluid cushion. The minute GFP- or FRP-positive rectal tumors were then surgically removed.

For pathological evaluation of lymph node metastasis, mice were sacrificed and all para-aortic or iliac lymph nodes were isolated and were stained with hematoxylin and eosin or were immunohistochemically analyzed.

In vivo *fluorescence imaging.* To monitor the outgrowth of the primary tumors and the metastatic lymph nodes, *in vivo* fluorescence images were obtained at laparotomy using an Olympus SZX16 microscope and a DP71

camera (Olympus, Tokyo, Japan). Images were processed for contrast and brightness with the use of Adobe Photoshop software (Adobe). Green fluorescence intensity was analyzed using Image J software for the quantification of lymph node metastasis. For long-term evaluation, abdominal images were serially obtained and quantified.

Quantitative real-time PCR analysis. We previously established a highly sensitive quantitative assay that targets a human-specific *Alu* sequence in order to quantify lymph node metastasis in mice. We used this previously described assay in this study to measure the number of metastatic human tumor cells in mouse lymph nodes[38]. Briefly, genomic DNA was extracted from harvested lymph node tissues and analyzed by the quantitative real-time PCR assay using a set of human *Alu* primers (sense: 5′-CTG AGG TCA GGA GTT CGA G-3′; and antisense: 5′-TCA AGC GAT TCT CCT GCC-3′). We also amplified the mouse *GAPDH* genomic DNA sequence using mouse *GAPDH* primers (sense: 5′-CCA CTC TTC CAC CTT CGA T-3′; and antisense: 5′-CAC CAC CCT GTT GCT GTA-3′). The number of metastatic tumor cells in mouse lymph nodes is defined as the *Alu*/*GAPDH* ratio relative to that of the PBS-treated sample (PBS = 1).

Immunohistochemistry. For histological studies, rectal tumors and lymph nodes were removed and placed into buffered formalin for 24 hours at room temperature. All of the tissues were subsequently processed through alcohol dehydration and paraffinization. Tissues were embedded in paraffin and sectioned for hematoxylin-eosin staining and also for immunohistochemical examination. After deparaffinization and rehydration, antigen retrieval was performed by microwave irradiation in 10 mmol/l citrate buffer (pH 6.0). Following quenching of endogenous tissue peroxidase, tissue sections were incubated with mouse anti-adenovirus type 5 E1AmAb (BD Biosciences). The sections were then incubated using the Histofine Mouse Stain Kit (Nichirei Biosciences, Tokyo, Japan) for 10 minutes at 25 °C to block nonspecific reactivity with mouse serum. Immunoreactive signals were visualized by using a 3,39-diaminobenzidine tetrahydrochloride solution, and the nuclei were counterstained with hematoxylin. Signals were viewed under a microscope (BX50; Olympus).

Statistical analysis. We used Student's *t*-test to identify statistically significant differences between groups. All data are expressed as means ± SD. *P* values less than 0.05 were considered statistically significant.

SUPPLEMENTARY MATERIAL

Figure S1. Schematic DNA structures of the telomerase-specific viruses.

Figure S2. *In vitro* cytopathic effect of OBP-301 on Colo205-GFP human colorectal cancer cells..

Figure S3. Procedure for inoculation of human colorectal cancer cells for establishment of a submucosally invaded orthotopic xenograft model.

Figure S4. *In vivo* lymphatic spread of a blue dye in the regional lymph nodes.

Figure S5. Removal of the primary rectal tumor mimicking endoscopic submucosal dissection (ESD).

Figure S6. Comparative study of OBP-301 and cisplatin effects in an orthotopic colorectal cancer xenograft model.

ACKNOWLEDGMENTS

We thank Tomoko Sueishi and Tae Yamanishi for their excellent technical support. We also thank Yoshiko Mori and Ryo Inada for helpful discussions. This work was supported in part by grants from The Mochida Memorial Foundation for Medical and Pharmaceutical Research (H.K.); The Kanae Foundation for the Promotion of Medical Science (H.K.); The 106th Annual Congress of the JSS Memorial Surgical Research Fund, Tokyo, Japan (H.K.) Young Scientists (B), The Ministry of Education, Culture, Sports, Science and Technology, Japan (H.K.), the Ministry of Education, Culture, Sports, Science, and Technology of Japan (T.F.) and the Ministry of Health, Labour and Welfare of Japan (T.F.). Y.U. is the president and CEO of Oncolys BioPharma, Inc., the manufacturer of viruses. H.T. and T.F. are consultants for Oncolys BioPharma, Inc. The other authors declare no conflict of interest.

REFERENCES

1. Yamamoto, H, Koiwai, H, Yube, T, Isoda, N, Sato, Y, Sekine, Y *et al.* (1999). A successful single-step endoscopic resection of a 40 millimeter flat-elevated tumor in the rectum: endoscopic mucosal resection using sodium hyaluronate. *Gastrointest Endosc* **50**: 701–704.
2. Repici, A, Hassan, C, De Paula Pessoa, D, Pagano, N, Arezzo, A, Zullo, A *et al.* (2012). Efficacy and safety of endoscopic submucosal dissection for colorectal neoplasia: a systematic review. *Endoscopy* **44**: 137–150.
3. Montgomery, M, Fukuhara, S, Karpeh, M and Brower, S (2013). Evidence-based review of the management of early gastric cancer. *Gastroenterol Rep (Oxf)* **1**: 105–112.
4. Volk, EE, Goldblum, JR, Petras, RE, Carey, WD and Fazio, VW (1995). Management and outcome of patients with invasive carcinoma arising in colorectal polyps. *Gastroenterology* **109**: 1801–1807.
5. Kudo, S, Kashida, H, Nakajima, T, Tamura, S and Nakajo, K (1997). Endoscopic diagnosis and treatment of early colorectal cancer. *World J Surg* **21**: 694–701.
6. Mainprize, KS, Mortensen, NJ and Warren, BF (1998). Early colorectal cancer: recognition, classification and treatment. *Br J Surg* **85**: 469–476.
7. Nivatvongs, S (2000). Surgical management of early colorectal cancer. *World J Surg* **24**: 1052–1055.
8. Ando, N, Ozawa, S, Kitagawa, Y, Shinozawa, Y and Kitajima, M (2000). Improvement in the results of surgical treatment of advanced squamous esophageal carcinoma during 15 consecutive years. *Ann Surg* **232**: 225–232.
9. Gotoda, T (2007). Endoscopic resection of early gastric cancer. *Gastric Cancer* **10**: 1–11.
10. Nascimbeni, R, Burgart, LJ, Nivatvongs, S and Larson, DR (2002). Risk of lymph node metastasis in T1 carcinoma of the colon and rectum. *Dis Colon Rectum* **45**: 200–206.
11. Wang, HS, Liang, WY, Lin, TC, Chen, WS, Jiang, JK, Yang, SH *et al.* (2005). Curative resection of T1 colorectal carcinoma: risk of lymph node metastasis and long-term prognosis. *Dis Colon Rectum* **48**: 1182–1192.
12. Takeuchi, H and Kitagawa, Y (2013). Sentinel node navigation surgery in patients with early gastric cancer. *Dig Surg* **30**: 104–111.
13. Kishimoto, H, Kojima, T, Watanabe, Y, Kagawa, S, Fujiwara, T, Uno, F *et al.* (2006). *In vivo* imaging of lymph node metastasis with telomerase-specific replication-selective adenovirus. *Nat Med* **12**: 1213–1219.
14. Burton, JB, Johnson, M, Sato, M, Koh, SB, Mulholland, DJ, Stout, D *et al.* (2008). Adenovirus-mediated gene expression imaging to directly detect sentinel lymph node metastasis of prostate cancer. *Nat Med* **14**: 882–888.
15. Liu, TC, Galanis, E and Kirn, D (2007). Clinical trial results with oncolytic virotherapy: a century of promise, a decade of progress. *Nat Clin Pract Oncol* **4**: 101–117.
16. Park, BH, Hwang, T, Liu, TC, Sze, DY, Kim, JS, Kwon, HC *et al.* (2008). Use of a targeted oncolytic poxvirus, JX-594, in patients with refractory primary or metastatic liver cancer: a phase I trial. *Lancet Oncol* **9**: 533–542.
17. Fujiwara, T (2009). Telomerase-specific virotherapy for human squamous cell carcinoma. *Expert Opin Biol Ther* **9**: 321–329.
18. Uchida, H, Marzulli, M, Nakano, K, Goins, WF, Chan, J, Hong, CS *et al.* (2013). Effective treatment of an orthotopic xenograft model of human glioblastoma using an EGFR-retargeted oncolytic herpes simplex virus. *Mol Ther* **21**: 561–569.
19. Kawashima, T, Kagawa, S, Kobayashi, N, Shirakiya, Y, Umeoka, T, Teraishi, F *et al.* (2004). Telomerase-specific replication-selective virotherapy for human cancer. *Clin Cancer Res* **10**(1 Pt 1): 285–292.
20. Hashimoto, Y, Watanabe, Y, Shirakiya, Y, Uno, F, Kagawa, S, Kawamura, H *et al.* (2008). Establishment of biological and pharmacokinetic assays of telomerase-specific replication-selective adenovirus. *Cancer Sci* **99**: 385–390.
21. Sasaki, T, Tazawa, H, Hasei, J, Kunisada, T, Yoshida, A, Hashimoto, Y *et al.* (2011). Preclinical evaluation of telomerase-specific oncolytic virotherapy for human bone and soft tissue sarcomas. *Clin Cancer Res* **17**: 1828–1838.
22. Kojima, T, Hashimoto, Y, Watanabe, Y, Kagawa, S, Uno, F, Kuroda, S *et al.* (2009). A simple biological imaging system for viable human circulating tumor cells. *J Clin Invest* **119**: 3172–3181.
23. Takeshita, K, Tani, M, Inoue, H, Saeki, I, Havashi, S, Honda, T *et al.* (1997). Endoscopic treatment of early oesophageal or gastric cancer. *Gut* **40**: 123–127.
24. Kojima, T, Parra-Blanco, A, Takahashi, H and Fujita, R (1998). Outcome of endoscopic mucosal resection for early gastric cancer: review of the Japanese literature. *Gastrointest Endosc* **48**: 550–4; discussion 554.
25. Inoue, H, Fukami, N, Yoshida, T and Kudo, SE (2002). Endoscopic mucosal resection for esophageal and gastric cancers. *J Gastroenterol Hepatol* **17**: 382–388.
26. Borie, F, Plaisant, N, Millat, B, Hay, JM and Fagniez, PL; French Associations for Surgical Research (2004). Appropriate gastric resection with lymph node dissection for early gastric cancer. *Ann Surg Oncol* **11**: 512–517.
27. Blackburn, EH (1991). Structure and function of telomeres. *Nature* **350**: 569–573.
28. Kim, NW, Piatyszek, MA, Prowse, KR, Harley, CB, West, MD, Ho, PL *et al.* (1994). Specific association of human telomerase activity with immortal cells and cancer. *Science* **266**: 2011–2015.
29. Gu, J, Andreeff, M, Roth, JA and Fang, B (2002). hTERT promoter induces tumor-specific Bax gene expression and cell killing in syngenic mouse tumor model and prevents systemic toxicity. *Gene Ther* **9**: 30–37.
30. Christiansen, A and Detmar, M (2011). Lymphangiogenesis and cancer. *Genes Cancer* **2**: 1146–1158.
31. Goel, S, Duda, DG, Xu, L, Munn, LL, Boucher, Y, Fukumura, D *et al.* (2011). Normalization of the vasculature for treatment of cancer and other diseases. *Physiol Rev* **91**: 1071–1121.
32. Hagendoorn, J, Tong, R, Fukumura, D, Lin, Q, Lobo, J, Padera, TP *et al.* (2006). Onset of abnormal blood and lymphatic vessel function and interstitial hypertension in early stages of carcinogenesis. *Cancer Res* **66**: 3360–3364.

33. Kume, K (2014). Endoscopic therapy for early gastric cancer: standard techniques and recent advances in ESD. *World J Gastroenterol* **20**: 6425–6432.
34. Uraoka, T, Saito, Y, Yamamoto, K and Fujii, T (2009). Submucosal injection solution for gastrointestinal tract endoscopic mucosal resection and endoscopic submucosal dissection. *Drug Des Devel Ther* **2**: 131–138.
35. Yamasaki, Y, Tazawa, H, Hashimoto, Y, Kojima, T, Kuroda, S, Yano, S *et al.* (2012). A novel apoptotic mechanism of genetically engineered adenovirus-mediated tumour-specific p53 overexpression through E1A-dependent p21 and MDM2 suppression. *Eur J Cancer* **48**: 2282–2291.
36. Nemunaitis, J, Tong, AW, Nemunaitis, M, Senzer, N, Phadke, AP, Bedell, C *et al.* (2010). A phase I study of telomerase-specific replication competent oncolytic adenovirus (telomelysin) for various solid tumors. *Mol Ther* **18**: 429–434.
37. Fujiwara, T, Tanaka, N, Kanazawa, S, Ohtani, S, Saijo, Y, Nukiwa, T *et al.* (2006). Multicenter phase I study of repeated intratumoral delivery of adenoviral p53 in patients with advanced non-small-cell lung cancer. *J Clin Oncol* **24**: 1689–1699.
38. Kojima, T, Watanabe, Y, Hashimoto, Y, Kuroda, S, Yamasaki, Y, Yano, S *et al.* (2010). *In vivo* biological purging for lymph node metastasis of human colorectal cancer by telomerase-specific oncolytic virotherapy. *Ann Surg* **251**: 1079–1086.
39. Kishimoto, H, Urata, Y, Tanaka, N, Fujiwara, T and Hoffman, RM (2009). Selective metastatic tumor labeling with green fluorescent protein and killing by systemic administration of telomerase-dependent adenoviruses. *Mol Cancer Ther* **8**: 3001–3008.
40. Kishimoto, H, Aki, R, Urata, Y, Bouvet, M, Momiyama, M, Tanaka, N *et al.* (2011). Tumor-selective, adenoviral-mediated GFP genetic labeling of human cancer in the live mouse reports future recurrence after resection. *Cell Cycle* **10**: 2737–2741.
41. Yang, M, Reynoso, J, Jiang, P, Li, L, Moossa, AR and Hoffman, RM (2004). Transgenic nude mouse with ubiquitous green fluorescent protein expression as a host for human tumors. *Cancer Res* **64**: 8651–8656.
42. Bouvet, M, Tsuji, K, Yang, M, Jiang, P, Moossa, AR and Hoffman, RM (2006). *In vivo* color-coded imaging of the interaction of colon cancer cells and splenocytes in the formation of liver metastases. *Cancer Res* **66**: 11293–11297.

Viral transduction of the HER2-extracellular domain expands trastuzumab-based photoimmunotherapy for HER2-negative breast cancer cells

Kyoko Shimoyama, Shunsuke Kagawa, Michihiro Ishida, Shinichiro Watanabe, Kazuhiro Noma, Kiyoto Takehara, Hiroshi Tazawa, et al.

Breast Cancer Research and Treatment

ISSN 0167-6806

Breast Cancer Res Treat
DOI 10.1007/s10549-015-3265-y

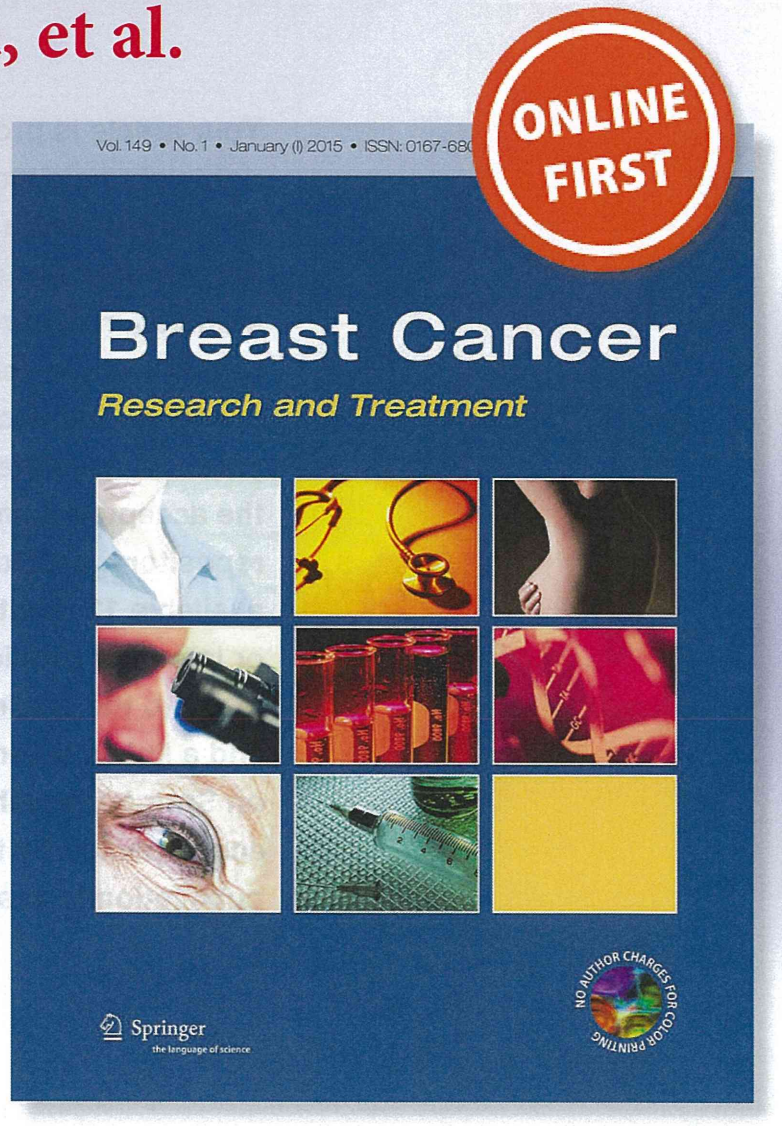

Springer